Multimedia Tools and Applications
https://doi.org/10.1007/s11042-019-7460-4

Automated detection of Glaucoma using deep learning convolution network (G-net)

Mamta Juneja[1] · Shaswat Singh[1] · Naman Agarwal[1] · Shivank Bali[1] · Shubham Gupta[1] · Niharika Thakur[1] · Prashant Jindal[1]

Received: 1 October 2018 / Revised: 7 January 2019 / Accepted: 7 March 2019
Published online: 03 April 2019

Abstract
Glaucoma is an ocular disease that is the leading cause of irreversible blindness due to an increased Intraocular pressure resulting in damage to the optic nerve of eye. A common method for diagnosing glaucoma progression is through examination of dilated pupil in the eye by expert ophthalmologist. But this approach is laborious and consumes a large amount of time, thus the issue can be resolved using automation by using the concept of machine learning. Convolution neural networks (CNN's) are well suited to resolve this class of problems as they can infer hierarchical information from the image which helps them to distinguish between glaucomic and non-glaucomic image patterns for diagnostic decisions. This paper presents an Artificially Intelligent glaucoma expert system based on segmentation of optic disc and optic cup. A Deep Learning architecture is developed with CNN working at its core for automating the detection of glaucoma. The proposed system uses two neural networks working in conjunction to segment optic cup and disc. The model was tested on 50 fundus images and achieved an accuracy of 95.8% for disc and 93% for cup segmentation.

Keywords Glaucoma detection · Optic disc · Optic cup · Retinal fundus image · Neural network · Image segmentation

1 Introduction

Glaucoma, also known as "silent thief of sight" is the second leading cause of blindness across the world. Over 60 million people suffer from glaucoma globally and by 2020, this number is expected to rise to 79.6 million [27]. It is characterized by the malfunctioning and loss of ganglion cells, which results in the change of the structure of the optic nerve head, the thickness of retinal nerve fiber layer, ganglion cell, and inner plexiform layers. Without proper treatment, glaucoma can cause irreversible damage to

✉ Prashant Jindal
jindalp@pu.ac.in

Extended author information available on the last page of the article

the optic nerve leading to permanent loss of vision. Thus, early diagnosis of glaucoma in the initial stages has been shown to significantly reduce the risk of permanent blindness [20].

The central circular yellowish region of the retina is referred to as the optic disc. This is the location where millions of retinal nerve fibers that carry visual signals from the eye to the brain converge and exit the retina. The optic disc is devoid of rods and cones which are photoreceptors that are responsible for vision. Hence, the optic disc is often termed as the "blind spot" of the eye. The optic disc has a central portion called the optic Cup. The optic cup is a relatively smaller bright cup-like area located at the centre of the optic disc [28]. In healthy adults, the optic cup covers nearly 30% of the optic disc [5].

Fundus image is an image of the eye obtained through a special fundus camera. This image shows the features of the fundus region including fovea, macula, optic disc and optic cup as depicted in Fig. 1 [2]. It is a non-invasive technique that has proven to be an effective tool for examining the ocular health of an individual.

In colored fundus images, the optic disc appears as a bright yellowish region and can be further subdivided into two parts namely the optic cup (inner part) and the neuroretinal rim (outer boundary). A glaucomatous eye can be identified by the optic nerve cupping i.e. the increase in the size of the optic cup. The best indicator for the detection of glaucoma is the cup-to-disc ratio (CDR), it is defined as the ratio of optic cup to optic disc diameter. A CDR value greater than 0.65 [13] is classified as glaucomic eye as per the clinicians. The

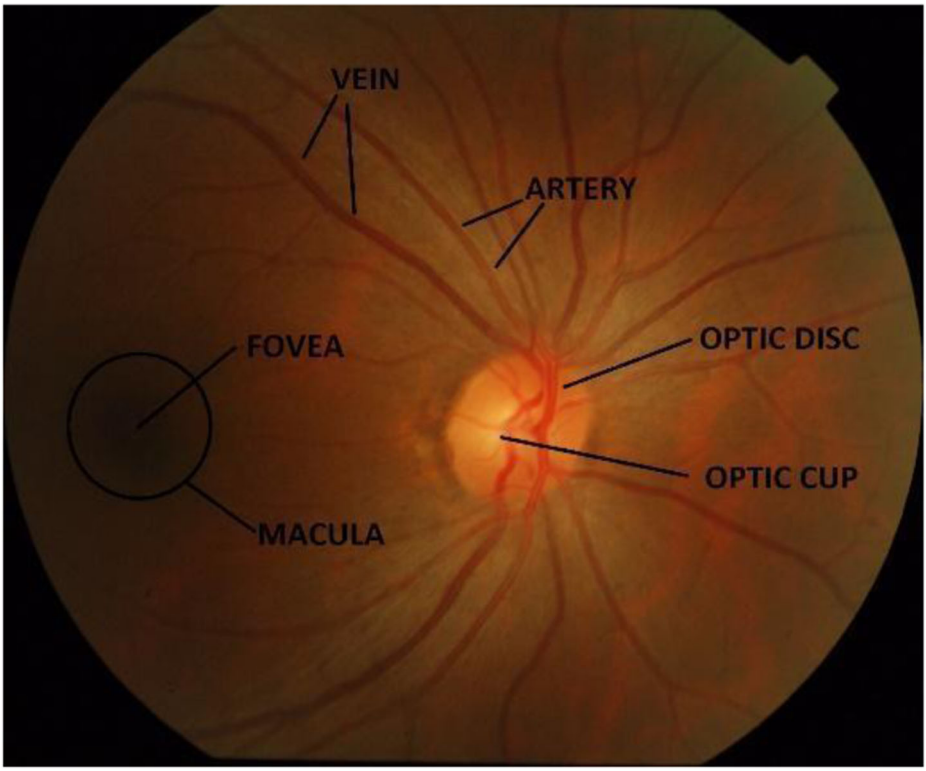

Fig. 1 A fundus image showing various features of the eye

methods by the doctors are very tiresome, time-consuming and inefficient as they need to manually segment out the discs and cups from individual images. Thus, there is a need for an automated diagnosis system for glaucoma to overcome the drawbacks of traditional methods [26]. It takes a skilled grader an average of about 8 min per eye to measure, record and subsequently diagnose whether the patient suffers from glaucoma. Automated methods using Computer-aided detection/diagnosis (CADe/CADx) system are therefore a better option for handling the segmentation problem. Figure 2 shows the representations of a healthy and a glaucomic eye.

CAD system comprises of three basic steps such as Pre-processing, Segmentation, and Classification [17]. Among these, pre-processing is the initial step used to remove outliers from the input image that create problems in further steps by reducing the accuracy of segmentation and classification. Removal of outliers or noise are performed by use of various filters such as mean, median and morphology depending on different modalities such as Computed Tomography (CT), Magnetic resonance imaging (MRI), and retinal images to get the desired region with improved accuracy [11, 18]. Thereafter, the segmentation is performed using different algorithms [12, 16, 19] to extract the desired region of interest and classify the abnormality.

Automated detection of glaucoma can be very useful in situations like mass screening where there is a scarcity of qualified doctors. As per the literature, there are many ways for glaucoma detection based on the analysis of Digital Fundus Images [33, 34]. In this paper, a Deep Learning architecture is proposed to differentiate glaucomatous eye from non-glaucomatous eye.

The proposed method involves:

1. Preprocessing the input images for removal of outliers. Firstly, the given image was cropped to remove the unnecessary part of the image. The cropped image was then passed through different filters to extract the useful information. Data augmentation was performed to increase the number of data points in the given dataset.
2. Feeding the filtered images to a neural network is used to segment the optic disc to remove the unnecessary part of the image as the optic cup resides inside the optic disc and cropped image is used for cup segmentation.

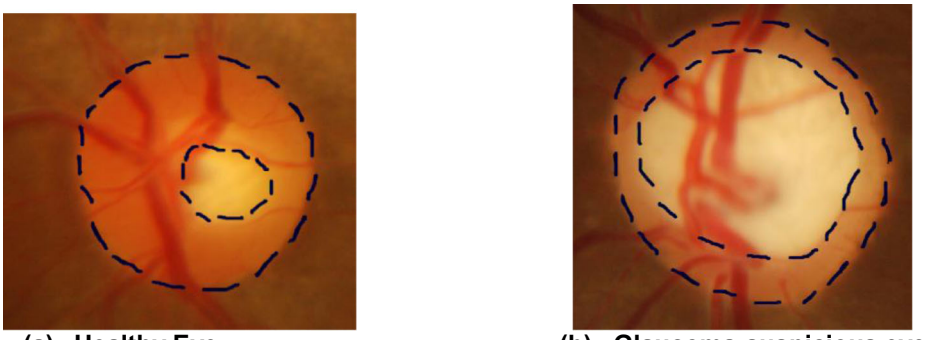

Fig. 2 Representations of healthy and glaucoma suspicious eyes from DRISHTI-GS database. The representations show the enlarged fundus images. The outer dashed lines encapsulate the optic disc whereas the inner dashed lines show the optic cup. Note that the CDR for a glaucoma suspicious eye is more than in the case of a healthy eye

3. Finding the value of CDR.
4. Predicting if a patient is progressing towards glaucoma or not.

This method is adopted because recent studies show that deep learning techniques have yielded highly discriminative representations and have helped in different computer vision tasks. In the network proposed above, we have used CNN as they work best for image classification and segmentation [32]. We have modified an existing neural network architecture used for image segmentation to increase the accuracy with which the model classifies an image as glaucomatous or non-glaucomatous. The success of deep learning algorithms in the field of medical imaging has motivated us to investigate these techniques and to apply those for the segmentation of cup and disc from fundus images.

The key feature of automated segmentation of optical regions is the recognition quality and prediction time. In order to be called a decision maker, a system should seldom make errors. Prediction time also plays an important role, especially when there is a need to segment a large number of images in a limited amount of time. Training time can be a concern if the algorithm is to be trained on a larger dataset. Otherwise, it is a one-time investment as we can use the pre-trained models for accurate prediction.

2 Dataset description

The DRISHTI-GS dataset [31, 32] consists of 101 images in total divided into two subsets: 50 Training images and 51 testing images. Training images are provided with ground truths for optic disc, optic cup and notching information. The testing set has 51 images for which ground truth is also available which can be used for validation.

The images were collected from Aravind eye hospital, Madurai, India from people visiting the hospital. The patients were classified as those having glaucoma and those with normal vision by clinical investigators on the basis of the diagnosis during examination. The subjects were 40–80 years of age, with an almost equal number of males and females. The images were dilated using the following data collection protocol: centered on optic disc with a Field-of-View of 30-degrees and of dimension 2896×1944 pixels and PNG uncompressed image format. The ground truth for each image was obtained by consulting four glaucoma experts having 3, 5, 9, and 20 years of experience, to capture interobserver variance in marking. The fundus region was extracted from the original image by eliminating the surrounding non-fundus mask region, to obtain an image of approximately 2047×1760 pixels. The ground truth for each image consists of manually marked region boundaries of the optic disc and optic cup.

3 Related work

A large number of attempts have been made to automate the segmentation of the optic disc and optic cup. The first step is to generalize the location of the optic disc as it needs to be isolated for further classification. This can be achieved as the optic disc tends to be brighter as compared to its surroundings, and is the site of origin for retinal blood vessels [31] [30]. Some of the approaches used till dates are as follows:

3.1 Optic disc segmentation

Optic disc is the location where the ganglion cell exits the eye which forms the optic nerve via which information from photoreceptors is transmitted to the brain. Some of the approaches used for segmentation to date are as follows. Initially, template-based methods were used for optic disc segmentation. In 2002 Walter et al. [36] proposed a method that used a modified variance image to detect the optic disc region and rim. They used watershed transform to find the contour of the optic disc and achieved an accuracy of 90%. In the same year, Chrástek et al. [10] gave a 4-step method for segmentation of the optic disc. This method involved the localization of optic disc, nonlinear filtering, Canny edge detector, and Hough transform. The results showed that the proposed algorithm was very robust. An accuracy of 97% was achieved for localization and 82% for segmentation. In the following year, Li et al. [21] proposed a method that localizes the optic disc using Principal Component Analysis (PCA) and detects the shape modified Active Shape Model (ASM). The accuracy for localization was 99% while for optic disc boundary detection was 94%.

Then in 2004, Lowell et al. [23] used the active contour model which detected the contour as per the image gradient using a special template matching technique. Tobin et al. [35] in 2006 proposed a method that used a probabilistic approach based on vasculature related properties of optic disc. A two-class Bayesian classifier which classified a pixel as optic disc or Not-optic disc was used. To further improve this technique, Kande et al. [15] proposed a method that used the concept of a point having maximum local variance which helps to compute the optic disc center. They used geometric active contour-based methods to find the boundary.

In 2010 Zhu et al. [39] proposed a method for detection of edges and boundaries to localize optic disc and its center. They used Sobel operators for detecting the edge and Hough transform for detecting the boundaries of localized optic disc. A success rate of 90% was achieved on the DRIVE database. In the subsequent year, Lu et al. [24] used Circular-based Transformation techniques to get the optic disc boundary. This technique captures the circular shape as well as the image variation over the boundary of optic disc with an accuracy of 99.75%. Circular Transformation used here combined detection of optic disc and segmentation in a single framework. At the same time, Liu et al. [22] used mathematical morphology and gradient vector flow snake model for localization and segmentation of optic disc in fluorescing retinal images. The accuracy for localization in this case, was observed to be 96.7% while the average sensitivity of 95.1% for images with defined optic disc.

In 2015 Chen et al. [7] proposed a deep CNN method named the ALADDIN (Automatic feature learning for glaucoma Detection based on Deep Learning) for learning features. Different from the traditional CNN, this method embeds micro neural networks with higher complexity in their structures to abstract the data present in the receptive field. In addition to that, a hierarchical representation is obtained for the fundus images to discriminate between glaucoma and non-glaucoma pattern. In the same year, another method for glaucoma detection based on deep neural networks was proposed by Chen et al. [8] which uses a 6 layered deep CNN to differentiate glaucomic from non-glaucomic images. Following this in 2016 Abdullah et al. [1] proposed a method based on the morphological operations, circular Hough transform and grow-cut algorithm. They used morphological operations for enhancing the optic disc and removed the pathologies. Circular Hough transform is used to approximate the optic disc center and finally, the grow-cut algorithm was applied to segment the optic disc boundary.

In 2017 Bharkad et al. proposed a method which used equiripple low pass finite impulse response (FIR) filter [6] which suppresses the concentration of the blood vessels in the optic disc region and improves the contrast. During the same year, Zahoor et al. [38] proposed a hybrid method for localization as well as segmentation of optic disc. Circular Hough Transform (CHT) was used for localization while Polar Transformation (PT) was used for segmentation.

3.2 Optic cup segmentation

Cup segmentation is a challenging task even for clinicians. The primary consideration of many methods is the bright pallor, which is a characteristic property of optic cup.

Wong et al. [37] proposed an automatic optic cup segmentation algorithm which is based on variational level set. This approach relies on the presence of the edge in the pallor region. The proposed method is a core component of ARGALI, a system for automated glaucoma risk assessment. Joshi et al. [14] used cup symmetry after applying thresholding to segment out the cup. However, due to the large variations in the intensity of the pallor region across patients, it made fixed thresholding technique inadequate for segmentation of cup. Another method proposed by Cheng et al. [9] uses a superpixel-based classification for segmentation of the cup. The major issue with this method is that it tends to favor medium-sized cups i.e. underestimating the large cups and overestimating the small ones.

Miri et al. [25] used a multimodel image segmentation method for segmentation of optical coherence tomography (OCT) and color fundus images. The disadvantage of this method was that it is dependent too much on the devices that take synchronized fundus and OCT images. These devices are very expensive and not so common.

Arnay et al. [4] proposed a new algorithm for segmentation of optic cup. They used Ant Colony Optimization meta-heuristics to achieve their goal. The meta-heuristic depends on the foraging behavior of ants. Pallor information and vessel curvature were combined using this algorithm.

Almazroa et al. [3] used type-II fuzzy thresholding approach and blood vessel extraction to segment the optic cup. First, the blood vessels were extracted using top-hat transform and Otsu's segmentation function which helped in detecting the curves in the blood vessels (kinks) that indicates the boundary of the cup. It was then followed by type-II fuzzy entropy procedure and Hough transform to approximate the boundary of the optic cup.

4 Methodology

Accurate detection of glaucoma through the proposed approach relies on the precise calculation of CDR, which in turn depends on accurate segmentation of optic disc and optic cup. Fig. 3 depicts the general flow for the proposed approach to make the input appropriate and manageable for a neural network. Preprocessing techniques applied to the input fundus images are:

4.1 Preprocessing

The pre-processing of the fundus images consists of the following step:

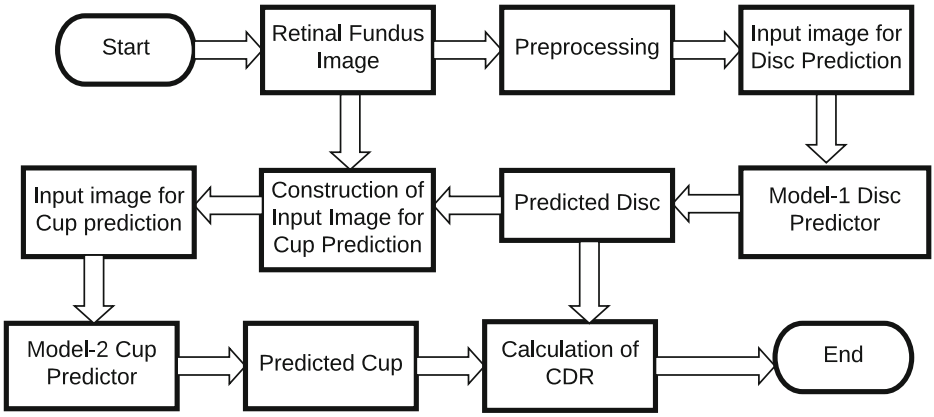

Fig. 3 Flow of the proposed algorithm

4.1.1 Cropping

The original fundus image with dimensions 2896 × 1944 was too large to directly feed to the neural network. Thus, to reduce the dimensionality of the original image, the relevant section consisting of the disc was cropped to 512 X 512 pixels. Cropping results in the loss of data, but since the approach used in this study is based on the CDR, the cropped-out section, which contains no portion of the cup or disc has no significant influence on the result of detection. Also, it reduces the computation time, increases the accuracy of segmentation and makes the input image uniform for further processing. Since the cup necessarily resides within the bounds of the disc, for segmentation of the cup, the mask obtained from disc segmentation was used to further crop the image to the size of the disc. Fig. 4 depicts the original fundus image, the cropped fundus image, and the segmented disc.

4.1.2 Channel separation

It was observed that the disc was most prominently observed in the Red channel of the RGB image. Therefore, the image was split into Red, Blue and Green channels and only the Red channel was used for segmentation of the disc, whereas for segmentation of the cup, best results were obtained by using all three RGB channels.

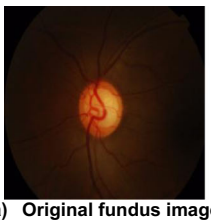

(a) Original fundus image

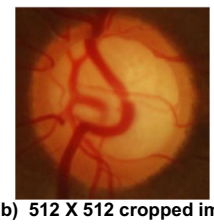

(b) 512 X 512 cropped image

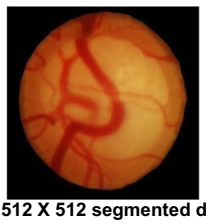

(c) 512 X 512 segmented disc

Fig. 4 The entire process of cropping

4.1.3 Data augmentation

The original dataset provided a limited number of 50 images usable as training data. This was insufficient to apply and train the neural network. Thus, to overcome this difficulty, rotation and flipping were applied as data augmentation techniques. The images were first flipped horizontally to double the size of the training set. Then all the images were flipped vertically which further increased the volume of the available data. After flipping, the images were rotated by an angle Θ. The angle of rotation Θ was increased from 0° to 180° with a step increment of 20°. This significantly increased the data size due to which the model was trained efficiently.

4.2 Segmentation using Glaucoma network (G-net)

The proposed method uses a modified version of U-net, which significantly increased the accuracy for segmentation of optic disc and cup. Two different CNNs were coded in python 3 using keras and opencv libraries for segmenting out the disc and cup separately. The first model was used to segment out the Optic disc. The inputs to the first model were the cropped retinal fundus images of size 512 X 512 pixels resized to 128 X 128 in the red channel. As the original images were of large sizes such as 2000 X 1600 pixels the CNN cannot be trained on those due to the requirement of high computation power, thus the size of the images was reduced to 128 X 128 pixels keeping the optic disc and cup at the centre. As the prominent visibility of the optic disc is in the red channel to segment out the disc, the model is trained on the red channel. The model has a total of 31 layers consisting of Convolutional(19), Maxpooling(4), Upsampling(4) and Merge layers(4). All the convolutional layers consist of filters of sizes (3,3) and (1,1) and the number of filters in the layers were 1,32 and 64 in the different layers. To reduce the loss of data across various layers the merge layers were used to merge previous layers with the upcoming layers. The maxpooling layer is used to select the maximum values from the clusters thus reducing the size of images. Upsampling layer upsamples the data by copying the same rows and columns in the images which were reduced due to the convolutional layers and maxpooling layers. The dropout layer was removed from the U-net model due to lack of dataset for the training of the proposed model. The model gives a mask of the optic disc, giving a black pixel if the corresponding pixel in the original image is segmented as optic disc, otherwise, a white pixel is given. To implement this, the last convolutional layer has a sigmoid activation function which gives either 1 or 0 for every input, whereas ReLU activation function is used for other layers. Thereafter, the model was trained on the batch size of 2 images for 500 epochs. From this model, the predicted images were saved and used for the training of the second model for segmenting out the cup.

The second CNN model is used to segment the cups from the retinal fundus images. As input, this model was provided with the optical discs of dimensions 512 X 512 cropped out of the original fundus image using segmentation masks output by the previous model. This significantly enhances the accuracy as the CNN analyses only the disc, which necessarily encloses the cup. It also helps in eliminating the major problem of finding the boundary of the optic cup as the boundary of the optic disc is more prominent than that of the optic cup thus making the detection of the optic cup easier. This model is similar to the previous with a total of 31 layers consisting of Convolutional, Maxpooling, Upsampling and Merge layer. Also, the model has the size of the filter in the convolution layer of dimensions (4,4) rather than (3,3) because of the

increased size of input images. This model gives the mask for the optic cup as output. The masks predicted by this model are saved. For the prediction of progression towards glaucoma, the images predicted by the first model are saved and using those mask images input for the second images are created. Fig. 5 shows the proposed architecture used to segment optic disc and optic cup.

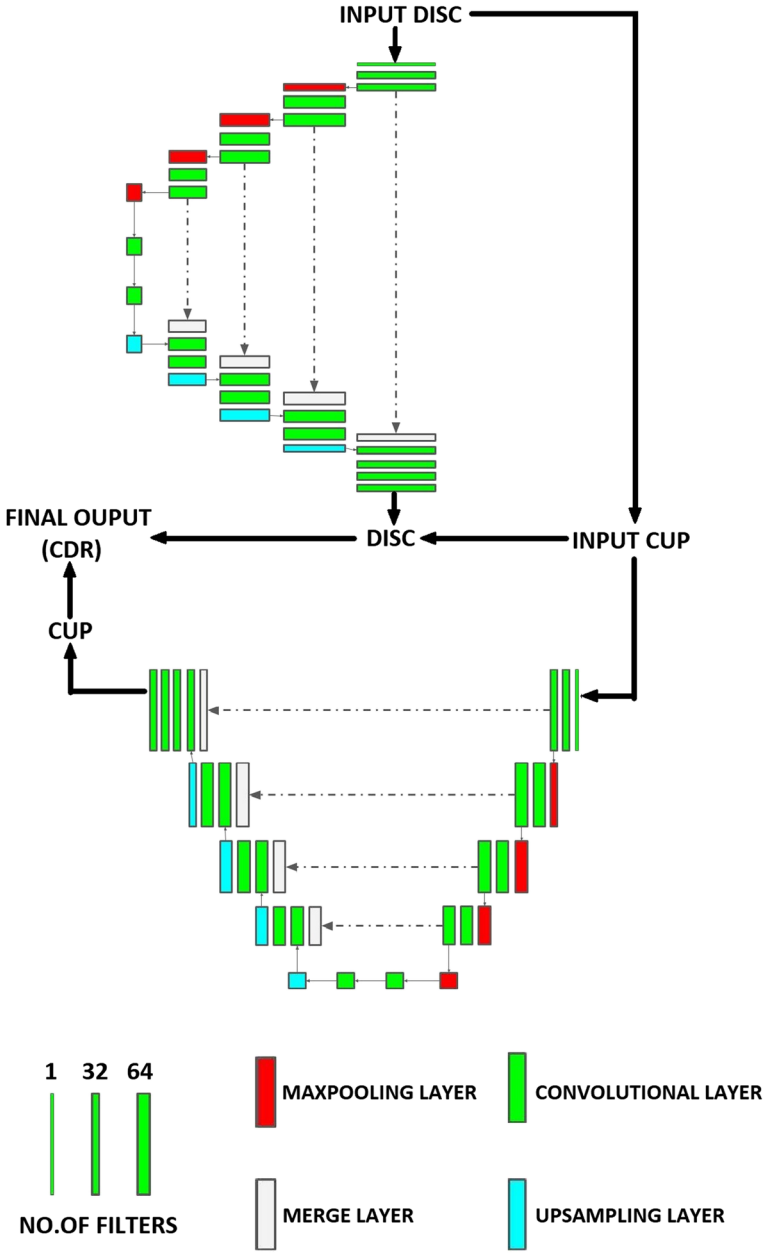

Fig. 5 G-Net architecture for segmentation of optic disc and optic cup

4.3 Designing and training

We have used a modified version of U-net for segmentation of optic disc and cup. The proposed architecture has increased the accuracy significantly. We have used two different CNNs in keras for segmenting out the disc and cup.

The first and second model segment out the optic disc and optic cup respectively. The input to the first model is the cropped retinal fundus images of size 512 X 512 pixels resized to 128 X 128 pixels in red channel. The model has a total of 31 layers consisting of Convolutional, Maxpooling, Upsampling and Merge layers. The second model is used for the segmentation of the cup from the input images. The input to this model is retinal fundus images of size 512 X 512 cropped according to the shape of the segmented disc. This is a similar model with total 31 layers consisting of Convolutional, Maxpooling, Upsampling and Merge layers with the difference in the size of model convolution layer of 4,4 rather than 3,3. A detailed description of the different layers along with their parameters consisting of the number of filters, size of filters and number of parameters is listed in Table 1.

4.4 Prediction

The aim of this study is to precisely obtain the radii ratio of cup over disk and predict the progression of Glaucoma. To obtain this ratio, we calculated the square root of the ratio of the areas of cup over disk. The number of white pixels in the segmented mask gives a measure of the areas of the discs and cups. We calculated the ratio of these areas. Subsequently, the square root of the ratio of these areas was calculated to obtain the required CDR. The CDR thus obtained was employed in predicting whether or not a patient is progressing towards glaucoma.

5 Results and discussion

The model was trained for optic disc and optic cup segmentation on a system with NVIDIA™ TITAN Xp 12 GB GDDR5X and 128 GB onboard RAM. It has a Xeon processor with 48 cores. The obtained results were quantified and compared with existing work [29]. For analysis and comparison of the segmentation results, seven metrics were used.

5.1 Accuracy metrics

5.1.1 Dice similarity coefficient

For two given sets X and Y, the Dice Similarity Coefficient (DSC) is calculated as

$$DSC = \frac{2|X \cap Y|}{|X| + |Y|} \tag{1}$$

where |X| and |Y| refers to the cardinality of sets X and Y respectively.

The same metric can be represented in terms of true positive, false positive and false negative as

Table 1 Description of all the layers present in the proposed network

Layer (type)	Parameters		
	No. of filters	Size of filters	Number of Parameters
conv2d_1Layers	32	3 × 3	896
conv2d_2	32	3 × 3	9248
max_pooling2d_1	–	2 × 2	0
conv2d_3	64	3 × 3	18,496
conv2d_4	64	3 × 3	36,928
max_pooling2d_2	–	2 × 2	0
conv2d_5	64	3 × 3	36,928
conv2d_6	64	3 × 3	36,928
max_pooling2d_3	64	2 × 2	0
conv2d_7	64	3 × 3	36,928
conv2d_8	64	3 × 3	36,928
max_pooling2d_4	64	2 × 2	0
conv2d_9	64	3 × 3	36,928
conv2d_10	64	3 × 3	36,928
up_sampling2d_1	–	2 × 2	0
concatenate_1	64	–	0
conv2d_11	128	3 × 3	73,792
conv2d_12	64	3 × 3	36,928
up_sampling2d_2	–	2 × 2	0
concatenate_2	128		0
conv2d_13	64	3 × 3	73,792
conv2d_14	64	3 × 3	36,928
up_sampling2d_3	–	2 × 2	0
concatenate_3	128		0
conv2d_15	64	3 × 3	73,792
conv2d_16	64	3 × 3	36,928
up_sampling2d_4	–	2 × 2	0
concatenate_4	96	–	0
conv2d_17	32	3 × 3	27,680
conv2d_18	32	3 × 3	9248
conv2d_19	1	1 × 1	33
conv2d_20	34	4 × 2	850
conv2d_21	34	4 × 2	9282
max_pooling2d_5	–	4 × 4	0
conv2d_22	64	4 × 4	34,880
conv2d_23	64	4 × 4	65,600
max_pooling2d_6	–	4 × 4	0
conv2d_24	64	4 × 4	65,600
conv2d_25	64	4 × 4	65,600
max_pooling2d_7	–	4 × 4	0
conv2d_26	64	4 × 4	65,600
conv2d_27	64	4 × 4	65,600
max_pooling2d_8	–	4 × 4	0
conv2d_28	64	4 × 4	65,600
conv2d_29	64	4 × 4	65,600
up_sampling2d_5	–	4 × 4	0
concatenate_5	128	–	0
conv2d_30	64	4 × 4	131,136
conv2d_31	64	4 × 4	65,600
up_sampling2d_6	–	4 × 4	0
concatenate_6	128		0
conv2d_32	64	4 × 4	131,136
conv2d_33	64	4 × 4	65,600
up_sampling2d_7	–	4 × 4	0

Table 1 (continued)

Layer (type)	Parameters		
	No. of filters	Size of filters	Number of Parameters
concatenate_7	128	–	0
conv2d_34	64	4 × 4	131,136
conv2d_35	64	4 × 4	65,600
up_sampling2d_8	–	4 × 4	0
concatenate_8	98	–	0
conv2d_36	34	4 × 2	26,690
conv2d_37	34	4 × 2	9282
conv2d_38	1	1 × 1	35

$$DSC = \frac{2TP}{2TP + FP + FN} \tag{2}$$

5.1.2 Jaccard index or intersection over Union (IOU)

The Jaccard index is a statistical metric that quantifies the similarity of two finite sets. For two given finite sets A and B, it is calculated as

$$J(A,B) = \frac{|A \cap B|}{|A \cap B|} = \frac{|A \cap B|}{|A| + |B| - |A \cap B|} \tag{3}$$

5.1.3 If a and B are both empty sets, we define the J(a,B) = 1.F-score

F-Score is a tool for statistical analysis of binary classification.

$$F_1 = \frac{2}{\frac{1}{\text{recall}} + \frac{1}{\text{precision}}} = 2 \cdot \frac{\text{precision} \cdot \text{recall}}{\text{precision} + \text{recall}} \tag{4}$$

where precision is (referred as the positive predictive value) the ratio of the retrieved features over the relevant ones whereas, recall (also called sensitivity) is the fraction of the relevant instances over the total sample space.

5.1.4 Structural similarity

It is a method used for predicting the perceived quality of digital images and videos.

$$SSIM(x,y) = \frac{\left(2\mu_x\mu_y + c_1\right)\left(2\sigma_{xy} + c_2\right)}{\left(\mu^2{}_x + \mu^2{}_y + c_1\right)\left(\sigma^2{}_x + \sigma^2{}_y + c_2\right)} \tag{5}$$

Where μ_x is the average of x, μ_y is the average of y, $\sigma^2{}_x$ is variance of x, $\sigma^2{}_y$ is variance of y, σ_{xy} is covariance of x and y and c_1, c_2 are two variables that stabilize the division.

5.1.5 Pixel accuracy

$$Pixel\ Accuracy = \frac{TP + TN}{TP + TN + FP + FN} \tag{6}$$

TP is true positives pixel-wise aggregated, TN is true negative pixel-wise aggregated, FP is false positive pixel-wise aggregated, FN is false negative pixel-wise aggregated.

5.1.6 Cohen kappa

$$Cohen\ Kappa = \frac{Total\ Accuracy - Random\ Accuracy}{1 - Random\ Accuracy} \tag{7}$$

$$Total\ Accuracy = \frac{TP + TN}{TP + TN + FP + FN} \tag{8}$$

$$Random\ Accuracy = \frac{(TN + FP)\cdot(TN + FN) + (TP + FP)\cdot(TP + FN)}{(TN + FN + FP + FN)^2} \tag{9}$$

TP is true positives pixel-wise aggregated, TN is true negative pixel-wise aggregated, FP is false positive pixel-wise aggregated, FN is false negative pixel-wise aggregated.

5.1.7 Mathews correlation coefficient (MCC)

$$MCC = \frac{TP \times TN - FP \times FN}{\sqrt{(TP + FP)(TP + FN)(TN + FP)(TN + FN)}} \tag{10}$$

TP is true positives pixel-wise aggregated, TN is true negative pixel-wise aggregated, FP is false positive pixel-wise aggregated, FN is false negative pixel-wise aggregated. In order to perform the evaluation, we resized all the testing images to 512×512 pixels and fed them to the proposed model. The complete algorithm was implemented in Python 3 and the following results were computed:

In order to determine which color channels provide the highest accuracy, the G-Net model was trained and validated several times on the RGB images, red channel images, blue channel images, and green channel images. The dice metric obtained are tabulated in Table 2.

The Optic cup was most accurately predicted using the model trained on the RGB image and the Optic disc using the model trained on the red channel. This in agreement with the visual discernibility of optic cup and optic disc in the different channels as depicted in Fig. 6.

Table 2 Comparison of dice metric accuracy on different channels used for segmentation of cup and disc

Image channel(s) used	Disc accuracy	Cup accuracy
RGB	94.72	93.71
Red	95.33	85.78
Green	91.2	90.05
Blue	92.04	92.08

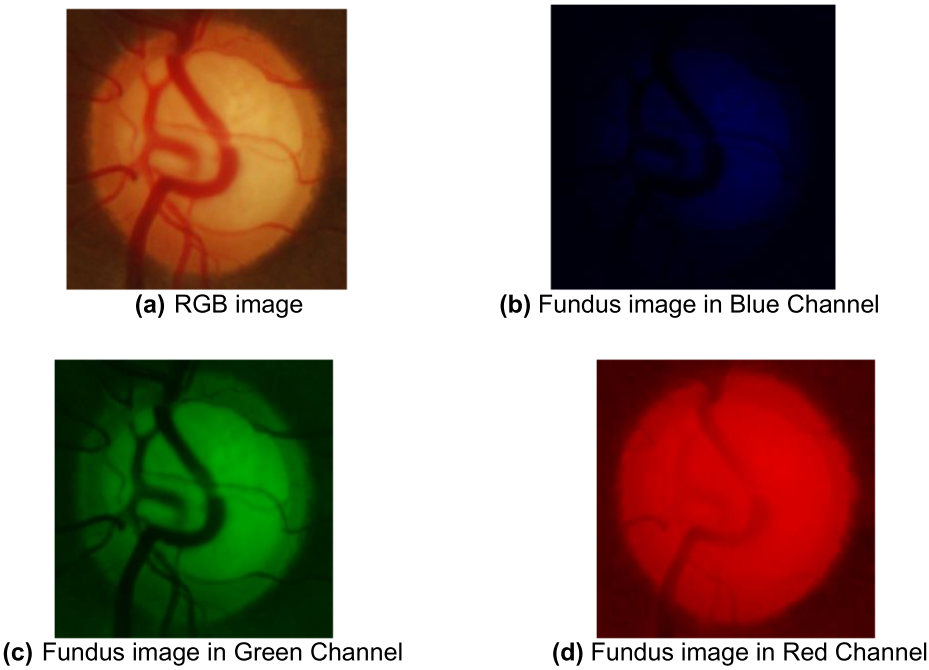

Fig. 6 Comparison of optic cup and optic disc in different channels

Table 3 and Fig. 7 indicate that the maximum accuracies for both cup and disc segmentation were obtained using the pixel accuracy metric. The best case and worst-case accuracies were calculated based on pixel accuracy. For disc segmentation, the best case resulted in an accuracy of 98.40% as depicted in Fig. 8. Figure 9 shows the worst case where accuracy of 80.17% was calculated.

For optic cup segmentation, the best case resulted in an accuracy of 96.77% as depicted in Fig. 10. Fig. 11 shows the worst case where an accuracy of 86.12% was calculated.

Table 3 Accuracy of disc and cup on various metrics

Accuracy Metric	Disc Accuracy (Red channel)	Cup Accuracy (RGB image)
Dice Metric	0.9505	0.9361
IOU	0.9062	0.8809
F1 score	0.9356	0.9162
Structural Similarity	0.8921	0.8690
Cohen Kappa	0.9110	0.8340
Pixel Accuracy	0.9586	0.9466
Matthews correlation coefficient (MCC)	0.9157	0.8454

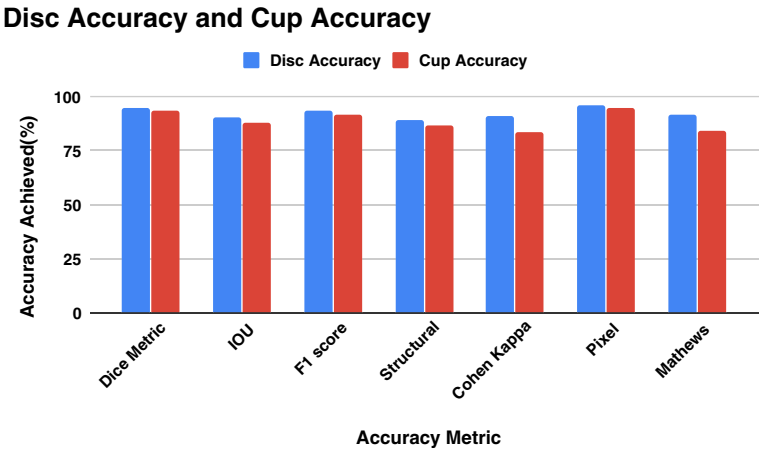

Fig. 7 Disc and cup accuracies on different metrics used in the experiment

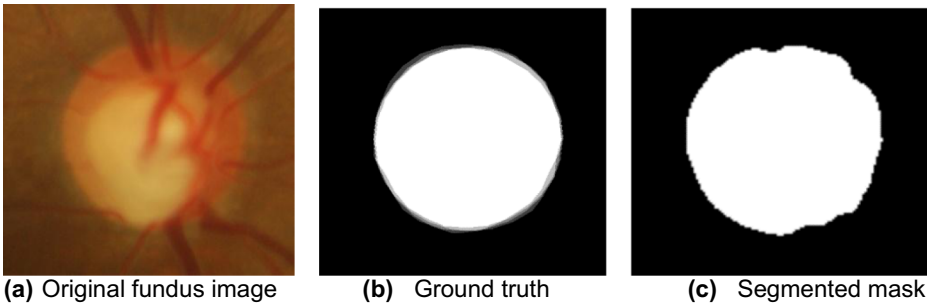

Fig. 8 Best case of optic disc segmentation

We compared the accuracy of the proposed model with different pre-existing approaches. A comparison of the Dice metric and IOU is shown in Table 4. The results clearly show that the proposed approach gives significantly better results than the other methodologies.

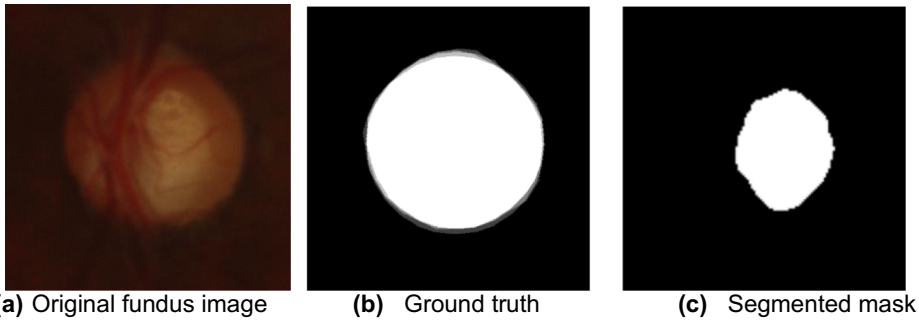

Fig. 9 Worst case of optic disc segmentation

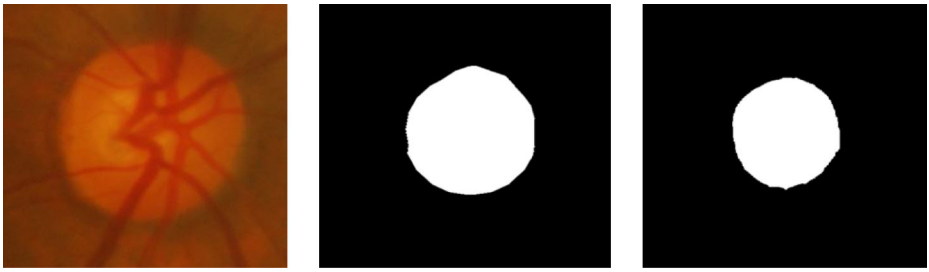

Fig. 10 Best case of optic cup segmentation

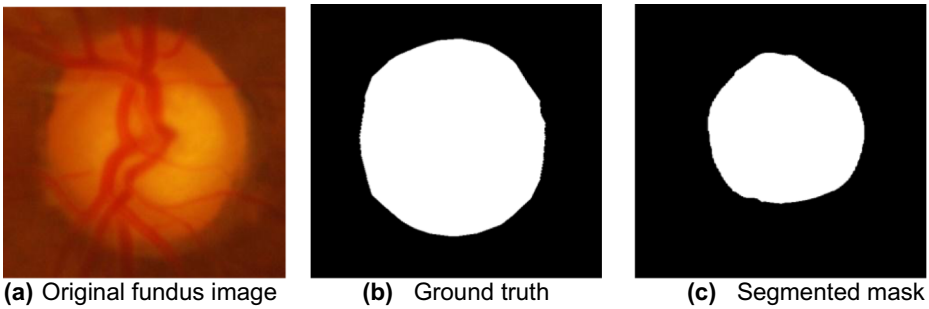

Fig. 11 Worst case of optic cup segmentation

Thus, the performance of the proposed approach for optic cup segmentation was compared with existing approaches on DRISHTI-GS dataset. The comparative analysis for same using Dice Metric and IOU is shown in Table 4 and Fig. 12. The proposed approach gave better results than the existing approaches. The values of Dice Metric for Artem [29], Zilly et al. (a) [40], Zilly et al. (b) [41] and the proposed approach were observed to be 0.85, 0.87, 0.83 and 0.93. Further, the IOU metric for Artem [29], Zilly et al. (a) [40], Zilly et al. (b) [41] and the proposed approach were found to be 0.75, 0.85, 0.86 and 0.88.

The architecture uses a combination of two neural networks that work in conjunction. The first network works on the preprocessed fundus image. The second network is fed on

Table 4 Comparison of different approaches used for segmentation of optic cup

Cup segmentation - DRISHTI-GS		
Approach	Dice Metric	IOU
Our approach	0.93	0.88
Artem[39]	0.85	0.75
Zilly et al. (a) [40]	0.87	0.85
Zilly et al. (b) [41]	0.83	0.86

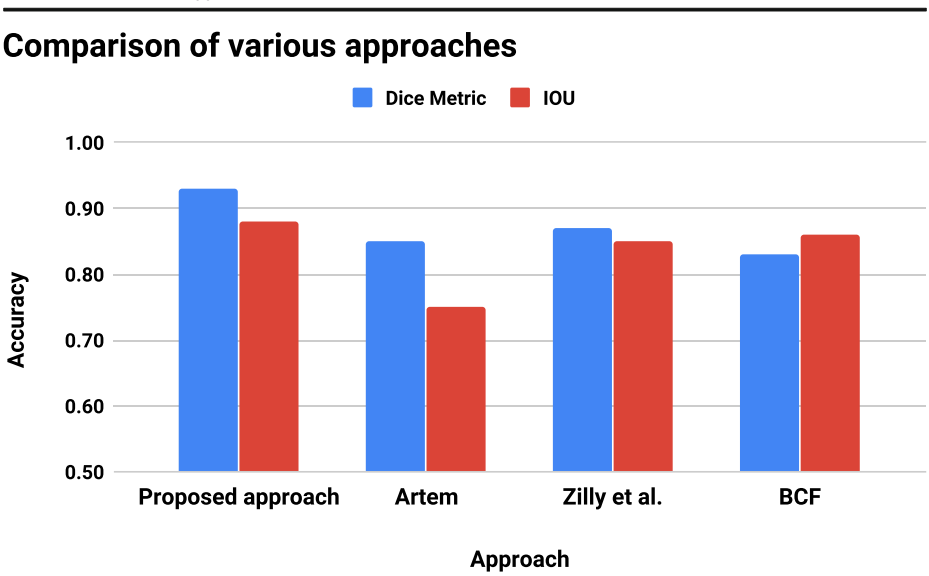

Fig. 12 Comparison of accuracy among different approaches

processed output from the first network. This output is used and built upon to generate the output of the second network. This concatenation of networks helps the architecture to achieve better accuracy compared to other approaches.

6 Conclusion

Glaucoma is a retinal disease that affects several people globally every year. Early detection is the only way to prevent its progression into permanent blindness. Since traditional methods require laborious manual inputs from ophthalmologists such as dimensions of disc and cup, the treatment often gets delayed. Hence it is essential to develop faster and more accurate methods for glaucoma detection. Automation provides a more viable and effective solution to this problem of glaucoma detection. The purpose of this proposed approach is to successfully segment optic cup and disc from a given fundus image. A proposed algorithm segments the Optic Disc and the Optic Cup from retinal fundus images using automated approach based on Deep Convolutional Neural Network architecture named as Glaucoma Network (G-Net). This algorithm consists of two neural networks working in conjunction to attain accuracies of 95.8% and 93.0% on OD and OC segmentation respectively. The architecture can be modified and applied to other medical images for a host of applications.

Acknowledgements The authors are grateful to the Ministry of Human Resource Development (MHRD), Govt. of India for funding this project under Design Innovation Centre (DIC) subtheme Medical Devices & Restorative Technologies (17-11/2015-PN-1). Dr. Prashant Jindal is currently working as Commonwealth Rutherford Fellow (CSC ID: INRF-2017-146) within the Medical Design Research Group Nottingham Trent University, Nottingham, UK and gratefully acknowledges the Commonwealth Scholarship Commission in the UK for their support.

References

1. Abdullah M, Fraz MM, Barman SA (2016) Localization and segmentation of optic disc in retinal images using circular Hough transform and grow-cut algorithm. PeerJ. 4:e2003
2. Algazi VR, Keltner JL, Johnson CA (1985) Computer analysis of the optic cup in glaucoma. Invest Ophthalmol Vis Sci 26(12):1759–1770
3. Almazroa A, Alodhayb S, Raahemifar K, Lakshminarayanan V (2017) Optic cup segmentation: type-II fuzzy thresholding approach and blood vessel extraction. Clinical ophthalmology (Auckland, NZ) 11:841
4. Arnay R, Fumero F, Sigut J (2017) Ant colony optimization-based method for optic cup segmentation in retinal images. Appl Soft Comput 52:409–417
5. Bach M (2001) Electrophysiological approaches for early detection of glaucoma. Eur J Ophthalmol 11(2_suppl):41–49
6. Bharkad S (2017) Automatic segmentation of optic disk in retinal images. Biomedical Signal Processing and Control 31:483–498
7. Chen X, Xu Y, Yan S, Wong DW, Wong TY, Liu J (2015) Automatic feature learning for glaucoma detection based on deep learning. InInternational Conference on Medical Image Computing and Computer-Assisted Intervention 2015 Oct 5 (pp. 669–677). Springer, Cham
8. Chen X, Xu Y, Wong DW, Wong TY, Liu J (2015) Glaucoma detection based on deep convolutional neural network. InEngineering in Medicine and Biology Society (EMBC), 2015 37th Annual International Conference of the IEEE 2015 Aug 25 (pp. 715–718). IEEE
9. Cheng J, Liu J, Xu Y, Yin F, Wong DW, Tan NM, Tao D, Cheng CY, Aung T, Wong TY (2013) Superpixel classification based optic disc and optic cup segmentation for glaucoma screening. IEEE Trans Med Imaging 32(6):1019–1032
10. Chrástek R, Wolf M, Donath K, Michelson G, Niemann H (2002) Optic disc segmentation in retinal images. InBildverarbeitung für die Medizin 2002 (pp. 263–266). Springer, Berlin, Heidelberg
11. Garg G, Juneja M (2018) A survey of denoising techniques for multi-parametric prostate MRI. *Multimedia Tools and Applications*, 1–34
12. Garg G, Juneja M (2018) A survey of prostate segmentation techniques in different imaging modalities. Current Medical Imaging Reviews 14(1):19–46
13. Goh KG, Hsu W, Lee ML, Wang H (2001) Adris: an automatic diabetic retinal image screening system. Studies in Fuzziness and Soft Computing 60:181–210
14. Joshi GD, Sivaswamy J, Karan K, Krishnadas SR (2010) Optic disk and cup boundary detection using regional information. InBiomedical Imaging: From Nano to Macro, IEEE International Symposium on 2010, (pp. 948–951). IEEE
15. Kande GB, Subbaiah PV, Savithri TS (2008) Segmentation of exudates and optic disk in retinal images. InComputer Vision, Graphics & Image Processing. ICVGIP'08. Sixth Indian Conference on 2008 Dec 16 (pp. 535–542). IEEE
16. Kaur R, Juneja M (2018) A survey of kidney segmentation techniques in CT images. Current Medical Imaging Reviews. 14(2):238–250
17. Kaur R, Juneja M, Mandal AK (2018) Computer-aided diagnosis of renal lesions in CT images: A comprehensive survey and future prospects. Computers & Electrical Engineering. 2018 Aug 22
18. Kaur R, Juneja M, Mandal AK (2018) A comprehensive review of denoising techniques for abdominal CT images. Multimedia Tools and Applications. 1–36
19. Kaur R, Juneja M, Mandal AK (2018) A hybrid edge-based technique for segmentation of renal lesions in CT images. Multimedia Tools and Applications. 1–21
20. Klein BE, Magli YL, Richie KA, Moss SE, Meuer SM, Klein R (1985) Quantitation of optic disc cupping. Ophthalmol. 92(12):1654–1656
21. Li H, Chutatape O (2003) A model-based approach for automated feature extraction in fundus images. Innull (p. 394). IEEE
22. Liu SP, Chen J (2011) Detection of the optic disc on retinal fluorescein angiograms. Journal of Medical and Biological Engineering 31(6):405–412
23. Lowell J, Hunter A, Steel D, Basu A, Ryder R, Fletcher E, Kennedy L (2004) Optic nerve head segmentation. IEEE Trans Med Imag 23(2):256–264
24. Lu S (2011) Accurate and efficient optic disc detection and segmentation by a circular transformation. IEEE Trans. Med. Imag. 30(12):2126–2133
25. Miri MS, Abràmoff MD, Lee K, Niemeijer M, Wang JK, Kwon YH, Garvin MK (2015) Multimodal segmentation of optic disc and cup from SD-OCT and color fundus photographs using a machine-learning graph-based approach. IEEE Trans Med Imaging 34(9):1854–1866
26. Pallawala P, Hsu W, Lee ML, Eong KGA (2004) Au-tomated optic disc localization and contour detection using ellipse fitting and wavelet transform, in ECCV, 2004, pp. 139–151

27. Quigley HA, Broman AT (2006) The number of people with glaucoma worldwide in 2010 and 2020. Br J Ophthalmol 90(3):262–267
28. Quigley HA, Broman AT (2006) The number of people with glaucoma worldwide in 2010 and 2020. Br J Ophthalmol 90(3):262–267
29. Sevastopolsky A (2017) Optic disc and cup segmentation methods for glaucoma detection with modification of U-net convolutional neural network. Pattern Recognition and Image Analysis 27(3): 618–624
30. Sharif Razavian A, Azizpour H, Sullivan J, Carlsson S (2014) CNN features off-the-shelf: an astounding baseline for recognition. In Proceedings of the IEEE conference on computer vision and pattern recognition workshops 2014 (pp. 806–813)
31. Sivaswamy J, Krishnadas SR, Joshi GD, Jain M, Tabish AU (2014) Drishti-gs: Retinal image dataset for optic nerve head (onh) segmentation. In 2014 IEEE 11th International Symposium on Biomedical Imaging (ISBI) (pp. 53–56). IEEE
32. Sivaswamy J, Krishnadas S, Chakravarty A, Joshi GD, Tabish AS (2015) A comprehensive retinal image dataset for the assessment of glaucoma from the optic nerve head analysis. JSM Biomedical Imaging Data Papers 2(1):1004
33. Thakur N, Juneja M (2017) Clustering based approach for segmentation of optic cup and optic disc for detection of Glaucoma. Current Medical Imaging Reviews 13(1):99–105
34. Thakur N, Juneja M (2018) Survey on segmentation and classification approaches of optic cup and optic disc for diagnosis of glaucoma. Biomedical Signal Processing and Control. 42:162–189
35. Tobin KW, Chaum E, Govindasamy VP, Karnowski TP, Sezer O (2006) Characterization of the optic disc in retinal imagery using a probabilistic approach. InMedical Imaging 2006: Image Processing (Vol. 6144, p. 61443F). International Society for Optics and Photonics
36. Walter T, Klein JC, Massin P, Erginay A (2002) A contribution of image processing to the diagnosis of diabetic retinopathy-detection of exudates in color fundus images of the human retina. IEEE Trans Med Imaging 21(10):1236–1243
37. Wong DW, Liu J, Lim JH, Jia X, Yin F, Li H, Wong TY (2008) Level-set based automatic cup-to-disc ratio determination using retinal fundus images in ARGALI. InEngineering in Medicine and Biology Society, EMBS 2008. 30th Annual International Conference of the IEEE 2008 Aug 20 (pp. 2266–2269). IEEE
38. Zahoor MN, Fraz MM (2017) Fast optic disc segmentation in retina using polar transform. IEEE Access 5: 12293–12300
39. Zhu X, Rangayyan RM, Ells AL (2010) Detection of the optic nerve head in fundus images of the retina using the hough transform for circles. J Digit Imaging 23(3):332–341
40. Zilly J, Buhmann JM, Mahapatra D (2017) Glaucoma detection using entropy sampling and ensemble learning for automatic optic cup and disc segmentation. Comput Med Imaging Graph 55:28–41
41. Zilly JG, Buhmann JM, Mahapatra D Boosting convolutional filters with entropy sampling for optic cup and disc image segmentation from fundus images. In: International workshop on machine learning in medical imaging 2015. Springer, Cham, pp 136–143

Dr. Mamta Juneja received her B.Tech., M.E. and Ph.D. degree in Computer Science and Engineering. She has been into the teaching profession since 2001 and has published more than 180 papers in refereed International Journals and conference proceedings with more than 790 citations in Google Scholar (with h-index of 12). She has served as a reviewer for many reputed journals. Presently, she is working as Assistant Professor in the Department of CSE, University Institute of Engineering. & Technology, Panjab University, Chandigarh, India. She is working on various research projects funded by MHRD and DeITY. Her research interests include Medical image processing, Biometric Security and Data Hiding.

Mr. Shaswat Singh is currently pursuing B.E in Computer Science and Engineering from University Institute of Engineering and Technology, Panjab University, Chandigarh. His research interests include artificial intelligence, machine learning, deep learning, image processing, and cryptography. He has extensively worked in the field of medical devices and restorative techniques, web development, Generative Adversarial Networks (GANs) and Convolutional Neural Networks (CNNs). He is currently working as a research intern at Design and Innovation Centre (DIC), UIET funded by MHRD.

Mr. Naman Agarwal is currently pursuing his B.E in Computer Science and Engineering from University Institute of Engineering and Technology, Panjab University, Chandigarh. His research interests include image processing, machine learning, and deep learning. He has extensively worked on Recurrent Neural Networks (RNN) and Convolutional Neural Network (CNN) and is currently working on Generative Adversarial Networks (GANS). He is currently working as a research intern at Design and Innovation Centre (DIC), UIET funded by MHRD.

Mr. Shivank Bali is currently pursuing B.E. degree in Computer Science and Engineering from University Institute of Engineering and Technology, Panjab University, Chandigarh, India. His research interests include Image processing, Deep Learning and Artificial Intelligence in fields such as Medical Imaging. Currently, he is working on projects at Design and Innovation Centre (DIC) Lab as a project intern funded by MHRD.

Mr. Shubham Gupta is currently pursuing his B.E. in the field of Computer Science from University Institute of Engineering and Technology, Panjab University, Chandigarh. He has done a great deal of research in the field of Medical Restorative Technologies under the wings of reputed researchers. His fields of interest are bioinformatics, machine learning, and artificial intelligence. He is currently working as a research intern at Design and Innovation Centre (DIC) funded by MHRD.

Ms. Niharika Thakur received her B.E and M.E degree in Computer Science and Engineering from University Institute of Engineering and Technology, Panjab university, Chandigarh in 2013 and 2015. Her research interests include medical image processing. She has published various papers in reputed international journals and conferences. Currently she is working as Ph.D. Research scholar in the Department of Computer Science and Engineering, UIET, Panjab University, India. She is also working on research project funded by MHRD and DeITY. Her research interest includes Medical image processing and restorative technologies.

Dr. Prashant Jindal received his B.Tech., M.Tech. and Ph.D. degree in Mechanical Engineering. He has been into the teaching profession since 2003 and has published many papers in refereed International Journals and conference proceedings. He is working as Assistant Professor in the Department of Mechanical engineering, University Institute of Engineering. & Technology, Panjab University, Chandigarh, India. Currently, he is also working as Commonwealth Rutherford Fellow within the Medical Design Research Group Nottingham Trent University, Nottingham, UK. He is also working on various research projects funded by MHRD and DRDO. His research interest includes Medical devices and Restorative technologies.

Affiliations

Mamta Juneja[1] · Shaswat Singh[1] · Naman Agarwal[1] · Shivank Bali[1] · Shubham Gupta[1] · Niharika Thakur[1] · Prashant Jindal[1]

Mamta Juneja
mamtajuneja@pu.ac.in

Shaswat Singh
shaswats.007@gmail.com

Naman Agarwal
namanagarwal8968@gmail.com

Shivank Bali
shivank565@gmail.com

Shubham Gupta
sbhmgupta17@gmail.com

Niharika Thakur
niharikathakur04@gmail.com

[1] University Institute of Engineering and Technology, Panjab University, Chandigarh, India